PERSPECTIVE

Dalton
www.rsc.org/dalton

The design of fluorescent sensors for anions: taking profit from the metal–ligand interaction and exploiting two distinct paradigms

Luigi Fabbrizzi,* Maurizio Licchelli and Angelo Taglietti
Dipartimento di Chimica Generale, Università di Pavia, via Taramelli 12, I-27100 Pavia, Italy. E-mail: luigi.fabbrizzi@unipv.it; Fax: +39 0382 528544; Tel: +39 0382 507328

Received 15th April 2003, Accepted 27th May 2003
First published as an Advance Article on the web 27th June 2003

Fluorescent sensors are molecular systems consisting of a receptor moiety and of a fluorogenic fragment, which are capable of recognising a given analyte and signalling recognition through a variation of the emission intensity. The fluorogenic fragment responsible of the signal can be associated to the receptor either covalently or non-covalently, giving rise to two well distinct classes of fluoro-sensors and sensing paradigms. The design of fluorescent sensors is described, with a special attention to the sensing of anionic groups (including those of amino acids). In any case, it seems convenient that the receptor moiety contains one or more metal centres, which establish strong coordinative interactions with the envisaged anionic substrate. Selectivity is related to the energy of the metal–analyte interaction and can be achieved by taking profit of the concepts developed in more than one hundred years of coordination chemistry. As an example, recognition and sensing of the amino acid histidine is considered in detail, which is based on the attitude of the imidazole residue to deprotonate and bridge two M^{II} ions prepositioned at the right distance, within a defined coordinative framework (M = Cu, Zn).

Revisiting a classical experiment of photophysics

A restricted number of molecules exist that, when excited by light of a given wavelength, undergo prompt deactivation by emitting light of higher wavelength. This phenomenon, defined as *fluorescence*, is in general visually perceived and represents a fascinating aspect of the interaction of light with matter. More interestingly, from a chemical point of view, the emission of a fluorescent substance in solution can be extinguished through the addition of a given reagent. The process is defined *quenching* (of the fluorescence, of the excited state of the fluorophore) and is associated to the occasional collision of the reagent with the fluorogenic fragment: it happens that, during the very short period in which the two species remain in contact, the reagent establishes with the fluorophore a process, which deactivates the excited state in a non-radiative way, thus preventing emission. A classical example of fluorescence quenching in solution is provided by the interaction of anthracene (An) and *N*,*N*-dimethylaniline (DMA) in an ethanolic solution.[1] On addition of DMA, the intensity of the vibrationally structured emission spectrum of An progressively decreases, as shown in Fig. 1.

Then, in Fig. 2, the fluorescence intensity, I_F, at 400 nm, is plotted *vs*. equivalents of DMA (open triangles): it is seen that complete quenching of the emission (in a solution 3×10^{-5} M of An) requires the addition of a very large excess of DMA (up to 5000 equiv.).

Data fit well a Stern–Volmer kinetics, as shown by the linear plot shown in the inset of Fig. 1, I_o/I *vs.* [DMA]. This behaviour is that expected for a bimolecular process, with no permanent interaction between the two colliding particles. From a mechanistic point of view, quenching is due to the occurrence of an electron transfer (eT) process involving the excited fluorogenic fragment An* and the DMA molecule. In particular, one electron is transferred from the lone pair of the tertiary nitrogen atom of DMA to the half-filled π* molecular orbital of An*, according to the process: $An^* + DMA \longrightarrow An^- + DMA^+$ (see the molecular orbital scheme shown in Fig. 3, step 2).

Then, a back electron transfer takes place (step 3), which restores An and DMA in their original states. At the very end, the electron circulation of steps 2 and 3 has deactivated the excited state An*, with no emission of light. Occurrence of

Luigi Fabbrizzi was born in Florence in 1946. In 1969, he graduated in chemistry at the University of Florence, where, from 1972 to 1980, he was lecturer of inorganic chemistry. Since 1980, he has been Professor of Inorganic Chemistry at the University of Pavia. His main research interests are related to the supramolecular chemistry of transition metals, with a special regard to the control of molecular motions and self-assembling processes, and to the design of optical molecular sensors for ions and molecules.

Maurizio Licchelli was born in Lecce in 1959. He graduated in Chemistry at the University of Pavia in 1983. He was a researcher at Enichem R&D Laboratories in Milan until 1990, when he joined the Department of General Chemistry of the University of Pavia as a Research Associate. Since 2001 he has been Associate Professor in the same Department. His current interests include the design of luminescent molecular sensors for ions and biologically relevant analytes and the photophysics of metal-containing supramolecular systems.

Angelo Taglietti graduated in Chemistry from the University of Pavia, where he also obtained his PhD in 1996 with a thesis on "Electron Transfer Processes in Supramolecular Chemistry", under the supervision of Prof. Luigi Fabbrizzi. Since 1999, he has been working as a research associate in University of Pavia, and his current research is centred on the design of sensory systems for biologically relevant substrates and on the synthesis of simple molecular level devices.

Luigi Fabbrizzi Maurizio Licchelli Angelo Taglietti

DOI: 10.1039/b304172g

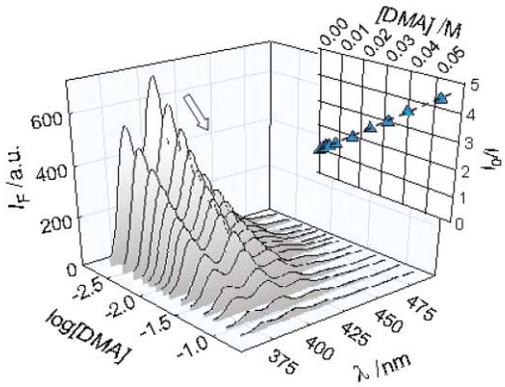

Fig. 1 Emission spectra recorded in the course of the titration of anthracene (An) with *N*,*N*-dimethylaniline (DMA) in an ethanolic solution. Fluorescence quenching is due to the occurrence of an electron transfer process from the the tertiary amine group of DMA to the excited fluorophore An*. Inset: Stern–Volmer plot associated to the titration experiment.

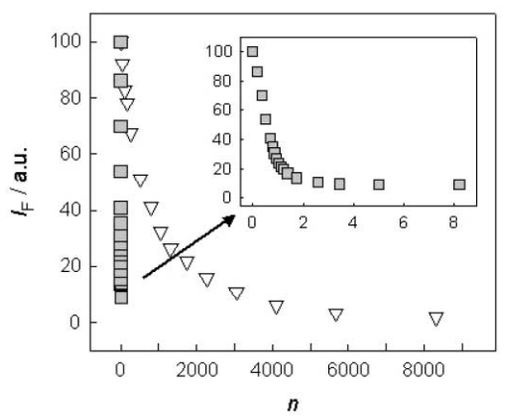

Fig. 2 Spectrofluorimetric profiles (i) for the titration of an ethanolic solution of anthracene (3×10^{-5} mol L^{-1}) with *N*,*N*-dimethylaniline (▽), emission spectra shown in Fig. 1, and (ii) for the titration of a methanolic solution of the $[Zn^{II}(\mathbf{1})]^{2+}$ complex (10^{-4} mol L^{-1}) with 4-*N*,*N*-dimethylaminobenzoate, **2** (■); the profile in the inset shows the 1 : 1 stoichiometry of the $[Zn^{II}(\mathbf{1})]^{2+}$/**2** adduct which forms.

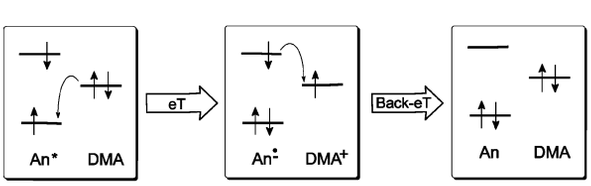

Fig. 3 Molecular orbital scheme illustrating quenching of excited anthracene (An*) through a photoinduced electron transfer from the tertiary nitrogen atom of *N*,*N*-dimethylaniline (DMA).

the crucial eT process can be accounted for on a thermodynamic basis. In particular, the free energy change associated to the electron transfer, ΔG°_{eT}, can be calculated from the combination of pertinent photophysical and electrochemical quantities, as shown in the thermodynamic cycle outlined in Fig. 4: the distinctly negative value (−0.6 eV) justifies the occurrence of the process.

The experiment is simple, it can be followed both visually and instrumentally, and it is well perceived and, due to the high sensitivity of fluorescence, can be monitored even at very low concentration of the reagents. Thus, one could ask whether it could be used in a practical context, for instance for analytical purposes. In this sense, anthracene should be the *sensor* and *N*,*N*-dimethylaniline the *analyte*. In this connection, it has to be noted that, in analytical chemistry, one would expect that the variation of the signalling property (*e.g.* switching ON OFF of the fluorescence) occurs at the 1 : 1 stoichiometric ratio of the

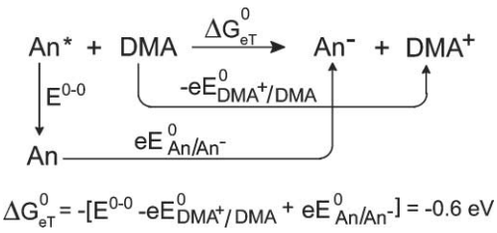

Fig. 4 Thermodynamic cycle for the electron transfer process from DMA to An. $E^{0\text{-}0}$, the photonic energy in eV, is obtained from the emission spectrum, E° values are electrode potentials and are obtained from pertinent electrochemical experiments.

reacting species. However, in the present case, a DMA : An ratio of 5000 : 1 and more is needed for the signal being switched OFF. This is essentially due to the statistical nature of the sensor–analyte interaction, which follows an occasional collision. Thus, in order to get an analytically convenient response, one should build permanent interactions with the aim of keeping anthracene and *N*,*N*-dimethylaniline in contact. In particular, we looked at metal–ligand interactions. In this sense, we first armed anthracene with the tripodal tetramine *tren*, to give **1** (see Scheme 1).[2]

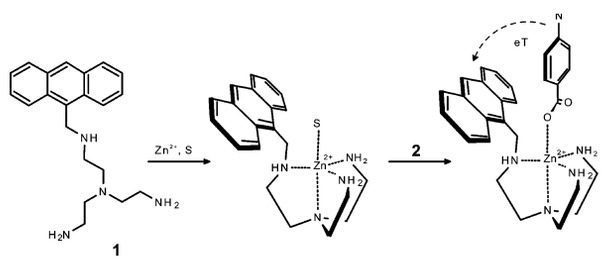

Scheme 1 Intra-complex electron transfer in the $[Zn^{II}(\mathbf{1})]^{2+}$/**2** adduct.

Then, on addition of the Zn^{II} ion, the corresponding tetramine chelate complex formed. The *tren* subunit typically imposes to Zn^{II} a trigonal bipyramidal coordination geometry, leaving one axial position available for the coordination of a further ligand, either an anion or a solvent molecule. On the other hand, we choosed a DMA framework equipped with the ligating group $-COO^-$, *N*,*N*-dimethylamine-4 benzoate, (**2**). A carboxylate subunit was chosen, as it displays enhanced binding tendencies towards coordinatively unsaturated Zn^{II}–polyamine complexes. Thus, an ethanolic solution of the $[Zn^{II}(\mathbf{1})]^{2+}$ complex was titrated with **2**. Before addition, the solution displayed the typical anthracene emission spectrum. Then, on addition of substoichiometric amounts of **2**, I_F was observed to decrease progressively, until almost complete quenching after the addition of one equiv. (grey squares in Fig. 2). The zoomed titration profile shown in the inset of Fig. 2 discloses the formation of a 1 : 1 adduct between $[Zn^{II}(\mathbf{1})]^{2+}$ and **2**. In particular, the value of the constant of the adduct formation equilibrium, determined through non-linear fitting of the titration profile, is 5.45 ± 0.03 log units.[2] Thus, in contrast to what observed for plain anthracene and *N*,*N*-dimethylaniline reactants, the $[Zn^{II}(\mathbf{1})]^{2+}$/**2** system operates under a strictly stoichiometric regime. This depends upon the fact that, following the coordinative interaction of the $-COO^-$ group with the Zn^{II} centre, the dimethylamine subunit is placed close enough to the anthracene fragment linked to the tren framework to allow the occurrence of a fast eT process.

Thus, under an analytical perspective, one could say that $[Zn^{II}(\mathbf{1})]^{2+}$ is a convenient *sensor* for the 4-*N*,*N*-dimethylaminobenzoate anion and, in general, for any benzoate ion bearing an electron donor (but also an electron acceptor) substituent. This does not seem an astonishing achievement in analytical chemistry. However, it can teach something useful for the design of fluorescent sensors and, in particular, help us to introduce the *'fluorophore–spacer–receptor'* paradigm.

The 'fluorophore–spacer–receptor' paradigm

The system $[Zn^{II}(\mathbf{1})]^{2+}$ is constituted by a receptor – the Zn^{II} tetramine complex subunit – which is there to interact with the analyte (to 'recognise', if the interaction with the analyte is very selective or specific) and by a fluorophore – the anthracene fragment – which is expected to modify its emission, following the setting up of the receptor–analyte interaction. Receptor and fluorophore are linked together by a $–CH_2–$ group, acting as a spacer. Thus, it is said that system $[Zn^{II}(\mathbf{1})]^{2+}$ has been built following a 'fluorophore–spacer–receptor' architecture.[3] Indeed, such an approach has been first introduced in order to design molecular sensors for s block cations,[4] and later extended to anion sensing.[5]

A crucial feature of fluorescent sensors is the way the signal is generated: the $[Zn^{II}(\mathbf{1})]^{2+}$ system is an ON OFF sensor, since, before recognition, anthracene displays its full emission (fluorescence ON), and recognition is signalled through the switching OFF of the fluorescence. In particular, it is the analyte itself that brings the signalling mechanism: it possesses donor properties and it is able to transfer one electron to the excited fluorophore, whose emission is quenched. In the following, we will try to show how the proper combination of the $[Zn^{II}(tren)]^{2+}$ and anthracene fragments, following the 'fluorophore–spacer–receptor' paradigm, can produce efficient sensors for natural amino acids.

It has been shown that the $[Zn^{II}(tren)]^{2+}$ platform is suitable for the recognition of analytes bearing a $–COO^-$ group. This class includes natural amino acids, of general formula $NH_3^+–CH(\mathbf{R})–COO^-$. However, if we look at selectivity, we cannot rely on the mere interaction of the Zn^{II} centre with the $–COO^-$ group, which is common to all the amino acids. Rather, we must equip the receptor framework with functionalities capable of establishing selective interactions with the **R** substituent of the envisaged amino acid. As an example, two anthracenyl groups and a benzyl group were appended to the external nitrogen atoms of the tripodal tetramine, to give **3**.[6]

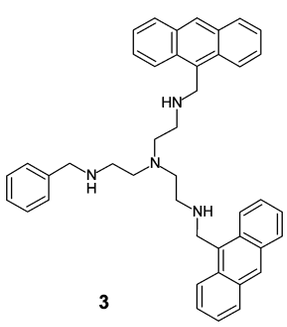

3

The aim was to create, in the corresponding $[Zn^{II}(\mathbf{3})]^{2+}$ complex, a hydrophobic cavity suitable for interaction with an **R** substituent bearing π characteristics.

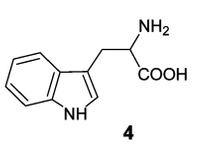

4

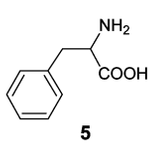

5

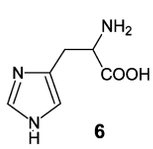

6

This points to the amino acids phenylalanine (TRP, **4**) and tryptophane (PHE, **5**). Notice that, in the $[Zn^{II}(\mathbf{3})]^{2+}$ system, each anthracene fragment also plays its usual role of fluorophore.

The interaction of $[Zn^{II}(\mathbf{3})]^{2+}$ with a variety of amino acids AA was preliminarily investigated through spectrophotometry by looking at the modifications of π–π* absorption bands observed when an ethanolic solution of $[Zn^{II}(\mathbf{3})]^{2+}$ was titrated with AA (note that AA indicates the zwitterionic form of the amino acid). In each case, the titration profile corresponded the the formation of a $[Zn^{II}(\mathbf{3})]^{2+}$/AA adduct of 1 : 1 stoichiometry. Then, the constants of the pertinent adduct formation equilibrium: $[Zn^{II}(\mathbf{3})]^{2+} + AA \rightleftharpoons [Zn^{II}(\mathbf{3})(AA)]^{2+}$ were determined through non-linear fitting of titration profiles. Indeed, the highest values were observed for PHE and TRP ($\log K = 4.48 \pm 0.05$ and 4.21 ± 0.02, respectively), to be compared with the values observed with glycine and other amino acids: around 3 log units in all cases. The higher stability of PHE and TRP adducts reflects the additional energy contribution provided by the π–π interaction between the aromatic groups on the tren framework and the **R** substituent of the amino acid (which correspond to an extra energy of 7–8 kJ mol^{-1}).

Then, a 10^{-4} M solution of the $[Zn^{II}(\mathbf{3})]^{2+}$ complex was put in the spectrofluorimetric cuvette and was titrated with the same amino acids. On titration, the fluorescent emission of anthracene remained unmodified with all amino acids but one: TRP. In particular, on addition of TRP, fluorescence intensity I_F was observed to decrease according to the profile shown in Fig. 5, open diamonds. Non-linear fitting of the titration profile disclosed the formation of a 1 : 1 adduct and the constant for the equilibrium: $[Zn^{II}(\mathbf{3})]^{2+} + TRP \rightleftharpoons [Zn^{II}(\mathbf{3})(TRP)]^{2+}$) was 4.28 ± 0.04 log units (in comfortable agreement with the value found through the spectrophotometric titration experiment). Molecular modelling studies performed on the $[Zn^{II}(\mathbf{3})(TRP)]^{2+}$ adduct suggest that the amino acid is bound to the zinc(II) polyamine receptor through two different interactions: (i) the metal–carboxylate coordinative interaction; (ii) an interaction of π nature, involving the indole residue of the amino acid and at least one of the anthracene substituents on the tetramine (see the sketch in Fig. 6).

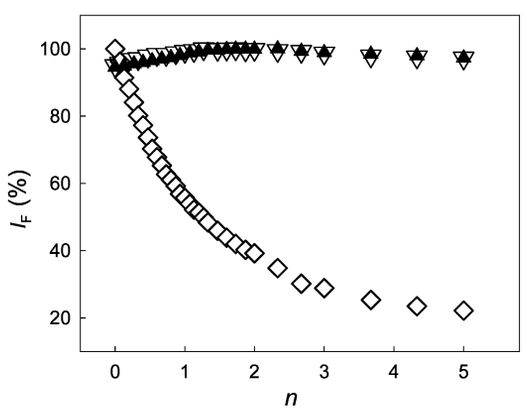

Fig. 5 Variation of the relative fluorescence intensity, I_F, of an ethanolic solution 10^{-5} M in $[Zn(\mathbf{3})]^{2+}$, when titrated with tryptophan (◇), phenylalanine (▲) and glycine (▽); n = number of equivalents of the added amino acid.

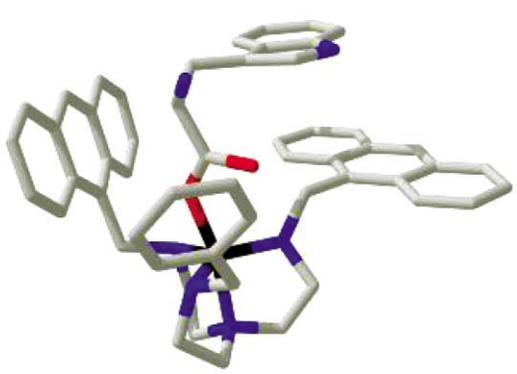

Fig. 6 Molecular model of the $[Zn(\mathbf{3})(TRP)]^{2+}$ adduct as obtained by using HyperChem package (MM+ force field). Hydrogens are omitted for clarity. Zn^{II} is in a trigonal-bipyramidal coordinative arrangement; the indole moiety of TRP and one of the anthracene subunits lie in parallel planes at a distance of 3.5–3.6 Å. This array is favourable to the occurrence of an electron transfer process from the indole fragment to the photoexcited anthracene subunit.

Thus, the observed quenching of the fluorescence is ascribed to the occurrence of an electron transfer (eT) process from the indole subunit (which behaves as an electron donor) to the photoexcited anthracene fragment (the acceptor). With the other amino acid bearing an aromatic fragment, PHE, an analogous π–π interaction should be established. However, in this case, as the substituent does not show any pronounced electron donor tendency, no electron transfer takes place to the excited anthracene fragment, whose emission is not modified. In conclusion, the $[Zn^{II}(\mathbf{3})]^{2+}$ complex, among natural amino acids, recognises PHE and TRP, on the basis of additional π–π interactions, but signals only the recognition of TRP through the switching OFF of the anthracene emission.

However, there exists a more direct way to generate selectivity in the interaction of a metal containing receptor with an amino acid NH_3^+–CH(**R**)–COO^-: the interaction of the metal with **R**. This may appear as a rather unprobable event in view of the typically scarce coordinative tendencies of **R** substituents of natural amino acids: however, there is at least one amino acid in which this possibility is given: histidine (**6**, HIS), whose **R** substituent is an imidazolyl group. In fact, very effective receptors for imidazole can be designed by taking profit of its tendency to deprotonate and to act as an ambidentate ligand towards metal ions. Imidazole, ImH, $pK_A = 14.5$, is a weaker acid than H_2O and does not deprotonate in water. However, in presence of two prepositioned metal ions M^{II}, the ImH molecule simultaneously deprotonate and the Im^- anion which forms bridges the two metal centres, according to a process described by the following equilibrium:

$$[M^{II}_2]^{4+} + ImH \rightleftharpoons [M^{II}(Im^-)M^{II}]^{3+} + H^+ \qquad (1)$$

A basic requirement for reaction (1) to proceed is that the two M^{II} centres occupy fixed positions, in a rigid coordinative framework, at the correct distance. This situation is present in nature, in the superoxide dismutase enzyme (SOD), in which the imidazolate group of a histidine residue bridges a Cu^{II} ion and a Zn^{II} ion. The metalloenzyme is supposed to eliminate the harmful radical O_2^-, through a disproportionation process which involves the Cu^{II}/Cu^{I} redox couple.[7] Artificial homodimetallic analogues of the heterodimetallic core of SOD have been prepared: either Cu^{II}, Cu^{II},[8] or Zn^{II}, Zn^{II}.[9] In most cases, the two metal ions are prepositioned in a two-compartment polyamine receptor and the two nitrogen atoms of the imidazolate bridging ligand complete the coordination sphere of each metal centre. On these bases, it was considered that a polyamine system containing two Zn^{II} ions could be a good candidate for imidazole recognition. At this stage, we excluded Cu^{II} derivatives, due the definite photophysical activity of this metal, which would quench any proximate excited fluorophore. Thus, we designed the homoditopic ligand **7**, in which two tren subunits are covalently linked by a 9,10-anthracenyl spacer (see the formula in Fig. 7).[10]

In aqueous solution, the bistren ligand **7** coordinates two Zn^{II} ions, to give the dinuclear complex $[Zn^{II}_2(\mathbf{7})]^{4+}$, which is present as a major species at pH = 7. Then, an imidazole molecule, when present in equimolar amount, deprotonates and goes to bridge the two Zn^{II} ions, giving the $[Zn^{II}_2(\mathbf{7})(Im^-)]^{3+}$ complex, which is the dominating species over the pH interval 9–10. The cascade process of Zn^{II} complexation and inclusion of Im^- is illustrated in Fig. 7. Therefore, the $[Zn^{II}_2(\mathbf{7})]^{4+}$ complex can behave as a receptor of imidazole in aqueous solution, and deserves to be tested as a fluorescent sensor for imidazole and the imidazole containing amino acid histidine.

Indeed, titration with imidazole of an aqueous solution of the $[Zn^{II}(\mathbf{7})]^{4+}$ complex, buffered at pH = 9.6, induced quenching of the anthracene fluorescence (see Fig. 8, open triangles). Non-linear fitting of the I_F *vs.* number of equivalents profile indicated the formation of the 1 : 1 receptor–analyte adduct,

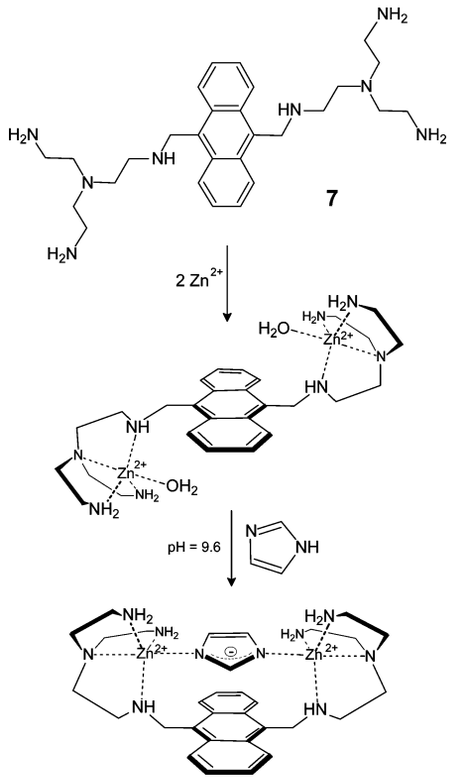

Fig. 7 Recognition and sensing of imidazole by a dinuclear zinc(II) complex. At pH = 9.6 imidazole deprotonates and bridges the two Zn^{II} centres of the dimetallic complex of the bistren ligand **7**. Then, within the $[Zn^{II}_2(\mathbf{7})(Im^-)]^{3+}$ complex, the electron rich imidazolate fragment transfers one electron to the proximate anthracene fragment, quenching its emission. The imidazole containing amino acid histidine is recognised and sensed through the same mechanism.

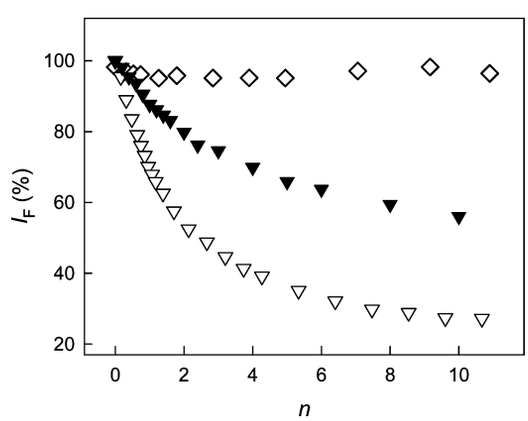

Fig. 8 Variation of the relative fluorescence intensity, I_F, in the course of the titration of an aqueous solution 10^{-5} M in the $[Zn^{II}_2(\mathbf{7})]^{4+}$ complex, buffered at pH = 9.6, with imidazole, ▽; histidine, ▼; and acetate, ◇; *n* = number of equivalents of the added analyte.

i.e. $[Zn^{II}(\mathbf{7})(Im^-)]^{3+}$, with a conditional equilibrium constant of 3.65 ± 0.04 log units.[10] Noticeably, titration with 1-methylimidazole, which cannot undergo deprotonation, did not induce any modification of the anthracene fluorescent emission, confirming that signalling is promoted by Zn^{II}–Zn^{II} bridging of the imidazolate fragment.

As far as photophysics is concerned, fluorescence quenching in the $[Zn^{II}(\mathbf{7})(Im^-)]^{3+}$ adduct has to be ascribed to the occurrence of an intra-complex electron transfer process from a π orbital of the electron rich Im^- moiety to a π* orbital of the photo-excited anthracene fragment. In Fig. 7, the anthracene subunit and the imidazolate fragment have been sketched as lying in parallel planes, a situation which should allow the overlap of the appropriate π orbitals and favour the occurrence of

the electron transfer process. Indeed, such a spatial arrangement has been shown to exist in the homologous dicopper(II) complex, $[Cu^{II}_2(\mathbf{7})]^{4+}$ whose crystal and molecular structure has been determined by X-ray diffraction studies.[11] The molecular structure of the imidazolate dicopper complex is shown in Fig. 9.

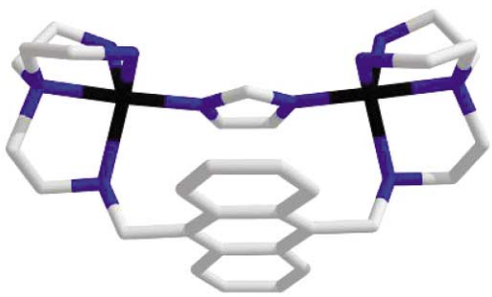

Fig. 9 The molecular structure (determined through X-ray diffraction studies) of the $[Cu^{II}_2(\mathbf{7})]^{4+}$ complex.[11] It is guessed that the homologous $[Zn^{II}_2(\mathbf{7})]^{4+}$ complex exhibits a similar structure. Under such circumstances, the almost parallel arrangement of the imidazolate ring (Im^-) and of the anthracene subunit (An) would account for the occurrence of an Im^--to-An* efficient electron transfer process.

Titration of the $[Zn^{II}(\mathbf{7})]^{4+}$ complex with histidine induced a fluorescence quenching similar to that produced by plain imidazole, but characterised by a lower value for the binding constant ($\log K = 2.92 \pm 0.01$, see Fig. 8, filled triangles): this may reflect the unfavourable contribution of the steric repulsions by the amino acid fragment Most interestingly, the titration profile is not modified when the solution contains even a large excess of any other amino acid. As an example, addition of histidine to a solution buffered at pH = 9.6 and containing the receptor $[Zn^{II}(\mathbf{7})]^{4+}$ plus 10 equiv. of glycine produced the same titration profile obtained in absence of the competing amino acid. Lack of interference may be due to the fact that the only anionic group any amino acid other than histidine can offer, *i.e.* the carboxylate fragment, does not display bridging tendencies toward the dimetallic core of $[Zn^{II}(\mathbf{7})]^{4+}$ receptor. For instance, titration with acetate did not alter at all the anthracene emission (see Fig. 8, open diamonds). Thus, $[Zn^{II}(\mathbf{7})]^{4+}$ behaves as a specific sensor of histidine, which is recognised and sensed in presence of any other natural amino acid.

At this stage, we can comment on the approach we have followed for the fluorescent sensing of amino acids and, in general, of anionic substrates. The choice of the metal–ligand interaction as a basis of the receptor-analyte binding seems beneficial. In particular, the energy of the metal–ligand interaction is quite high, high enough to compensate the endothermic contribution due to the desolvation of the anion. As a consequence, metal containing receptors can operate in highly polar and solvating media (in the examples shown before: aqueous ethanol for tryptophane sensing, pure water for histidine). This is not always the case for the receptors operating through the weaker electrostatic interactions (which include hydrogen bonding), whose utilisation is often confined to apolar or poorly polar solvents.[12]

The signalling side is perhaps less satisfactory. We followed the 'fluorophore–spacer–receptor' paradigm, which demands that a light-emitting subunit is synthetically connected to the ligating framework. Chemical manipulation requires that the fluorophore is thermally and chemically resistant (like anthracene) and discourages the employment of more sophisticated and more fragile fluorogenic fragments (as the majority of dyes emitting at 500 nm and more). A second point concerns with the signalling mechanism: the Zn^{II}–polyamine based sensor, either $[Zn^{II}(\mathbf{3})]^{2+}$ or $Zn^{II}_2(\mathbf{7})]^{4+}$, is *per se* fluorescent and waits for an analyte bringing with itself the quenching mechanism: in the considered examples, it was the capability to release one electron to the excited fluorophore, properly positioned on the receptor framework. This restricts successful sensing to analytes displaying electron donor (but also electron acceptor) tendencies and excludes the vast class of substrates which do not present any electron exchanging features. In this connection, we have observed the unpleasant situation of a system, $[Zn^{II}(\mathbf{3})]^{2+}$, which senses well TRP, but does not sense PHE, the other amino acid bearing an aromatic fragment. Actually, PHE is perfectly recognised, but is not fluorimetrically sensed because it does not exhibit any electron donor property. Last, but not least, we are not especially happy with the ON OFF switching mode of the envisaged systems: in fact, we would prefer that recognition is signalled through the revival of quenched fluorescence (the OFF ON mode). Or, at least, this is the common feeling of our colleagues cell physiologists, who make extensive utilisation of fluorescent sensors for monitoring the activity of a variety of analytes inside the cell (their beloved substrate is the Ca^{2+} ion). They use fluorescence microscopy as an analytical tool and a variation of the concentration of the envisaged analyte is perceived and recorded as a glowing spot in the computer monitor, whose intensity either increases or decreases. When planning together the design of a fluorescent sensor for a given analyte, a friend biologist told us: 'I prefer to watch a light-torch switching ON in the Black Forest, rather than to look for the light of an apartment switching OFF in the night in Manhattan'.[13] Definitively, he convinced us of the superiority of the OFF ON signalling mode.

On the basis of the arguments stated above, we are urged to move to a different paradigm. In particular, we look at systems which (i) do not require a tedious multistep synthesis, (ii) both recognise and sense the desired analyte, and (iii) signal the recognition through a sharp revival of the fluorescence of chosen fluorophores of varying nature and complexity.

The 'chemosensing ensemble' paradigm

The new sensing approach we want to follow makes use of an indicator, In. In particular, In is bound, not too strongly, to the receptor R, to give a kinetically labile [R–In] adduct. Then, the envisaged substrate S, displaying a special affinity for R, is added to the solution: S displaces from the receptor cavity the loosely bound In, which is released to the solution, according to the fast metathetic equilibrium (2):

$$[R–In] + S \rightleftharpoons [R–S] + In \qquad (2)$$

For signalling purposes, it is required that an optical property of the indicator, *e.g.* colour, distinctly changes, depending whether In is bound to R or is free. Under such circumstances, substrate recognition, and indicator release, will be signalled by a sharp colour change. This analytical procedure, which works in a manner similar to that of many antibody-based biosensors in competitive immunoassays,[14] has been recently revived by Anslyn, who designed a class of [receptor + optical indicator] systems, useful for anion recognition.[15] Making reference to the concerted performance of a group of musicians, Anslyn named the [R + In] system a 'chemosensing ensemble'. We have now to convert this paradigm to the fluorescent sensing of anions, based on the metal–ligand interaction.

First, the indicator should be a fluorogenic fragment and should be also able to coordinate the metal centre of the receptor: this goal can be achieved by using a $–COO^-$ containing fluorophore: the $–COO^-$ group displays distinct coordinating tendencies towards transition metal ions. Then, we must operate in such a way that the fluorescent emission changes drastically following the displacement of the indicator. In order to profit from the more valuable OFF ON signalling, it must happen that (i) the fluorophore is quenched when bound to the metal, and (ii) it displays its full fluorescence when released to the solution. In other words, the receptor must be able to

quench the fluorescent indicator. To do that, we must choose a photophysically active ('guilty') metal ion, instead of the photophysically inactive ('innocent') Zn^{II} centre used in the 'fluorophore–spacer–receptor' paradigm, as described in the previous Section. This could be the case of the Cu^{II} ion, which, due to the incomplete filling of the 3d level and to the definite redox activity, is inclined to quench any nearby fluorophore through either an energy transfer or an electron transfer process, respectively.[16] As an extra benefit, Cu^{II}, which is highest in the Irving–Williams series, gives the most stable complexes among divalent 3d metal ions.

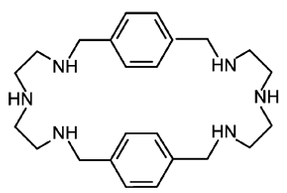

8

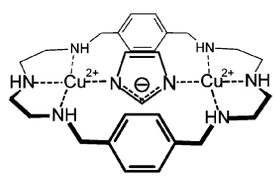

9

To test the outlined procedure, let us consider again the fluorescent detection of histidine. In the present case, the receptor must be a dinuclear complex of copper(II), containing coordinatively unsaturated metal centres. In particular, we considered the dimetallic complex of the the bis-dien macrocycle **8**, in which the two Cu^{II} centres are prepositioned at the right distance for imidazolate coordination. Indeed, on reaction of $[Cu^{II}_2(\mathbf{8})]^{4+}$ with imidazole in neutral solution, a stable imidazolate complex forms, $[Cu^{II}_2(\mathbf{8})(Im)]^{3+}$, whose molecular structure has been determined through X-ray diffraction studies,[17] and is sketched as formula **9**.

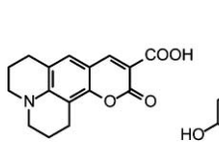

10

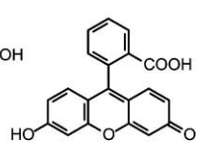

11

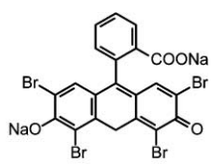

12

Thus, the $[Cu^{II}_2(\mathbf{8})]^{4+}$ complex was our promising receptor. Then, as a fluorescent indicator, we took from the shelf the following three dyes: coumarin 343 (**10**), fluorescein (**11**) and eosine Y (**12**), which share high quantum yield, excitation and emission wavelengths in the visible region, and the presence of a carboxylate group in the molecular structure. In particular, the $-COO^-$ group can act as a bridge for the two Cu^{II} centres of $[Cu^{II}_2(\mathbf{8})]^{4+}$. Titration experiments showed that the $[Cu^{II}_2(\mathbf{8})]^{4+}$ receptor, at pH = 7, binds each indicator, $R–COO^-$, and quenches its emission.[18] The association constants for the adduct formation equilibrium:

$$[Cu^{II}_2(\mathbf{8})]^{4+} + R–COO^- \rightleftharpoons [Cu^{II}_2(\mathbf{8})(R–COO)]^{3+} \quad (3)$$

vary to a substantial extent for the three indicators (log units: coumarin, 4.3; fluorescein, 5.9; eosine Y, 7.2).

Thus, the non-fluorescent chemosensing ensemble was generated by dissolving the $[Cu^{II}_2(\mathbf{8})]^{4+}$ receptor and the chosen fluorescent indicator in an aqueous solution buffered at pH = 7.[18] Notice that the indicator does not need to be equimolar with the receptor, but it has to be present at a concentration up to 100 times lower. Then, each receptor/indicator duo was titrated with HIS and with some representative amino acids, which could act as interferents: ALA, PHE, LEU, PRO and GLY. We observed a different behaviour depending upon the nature of the amino acid and of the indicator. In some cases, the amino acid was able to displace the indicator from the receptor, an event signalled by full fluorescence revival. In other cases, however, the amino acid was not able to dislodge the indicator, with no fluorescence restoring.

Some typical titration profiles are reported in Fig. 10. The $[Cu^{II}_2(\mathbf{8})]^{4+}$/coumarin duo (Fig. 10(a)) does not discriminate HIS and GLY. In fact, both HIS and GLY displace the indicator and restore its full emission. The situation is more favorable with the Fluorescein containing ensemble (Fig. 10(b)), which satisfactorily discriminates HIS (full recovering of fluorescence) from GLY, whose I_F profile is distinctly less steep. However, the highest sensing selectivity is observed with the $[Cu^{II}_2(\mathbf{8})]^{4+}$/eosine Y duo (Fig. 10(c)), which discriminates well HIS (full dispacement of the indicator and complete restoring of fluorescence) from GLY and other amino acids (which do not dislodge the indicator and do not revive fluorescence).

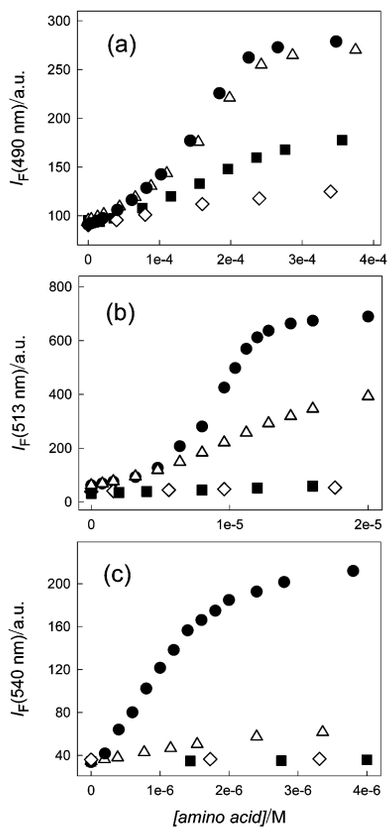

Fig. 10 Titration of the chemosensing ensemble $[Cu^{II}_2(\mathbf{8})]^{4+}$/Indicator (In) with selected amino acids (AA): (a) In = coumarin 343: 10^{-6} M, $[Cu^{II}_2(\mathbf{8})]^{4+} = 2.5 \times 10^{-4}$ M; (b) In = fluorescein: 10^{-6} M, $[Cu^{II}_2(\mathbf{8})]^{4+} = 1.6 \times 10^{-5}$ M; (c) In = eosine Y: 10^{-6} M, $[Cu^{II}_2(\mathbf{3})]^{4+} = 2.4 \times 10^{-6}$ M. AA: histidine (●); glycine (△); alanine (■); phenylalanine (◇).

In order to explain the selectivity pattern illustrated in Fig. 10, it is useful to consider the equilibrium constants for the interaction of $[Cu^{II}_2(\mathbf{8})]^{4+}$ with each amino acid, at pH = 7, as shown by the equation below:

$$[Cu^{II}_2(\mathbf{8})]^{4+} + AA \rightleftharpoons [Cu^{II}_2(\mathbf{8})(AA)]^{4+} \quad (4)$$

Values of the binding constants for each investigated amino acid AA are reported as bars in the diagram in Fig. 11.

As expected, the highest binding constant is shown by HIS, which offers to the two Cu^{II} centres the strongly donating imidazolate bridging group. Then, other amino acids come, which all interact with the metals of the receptor with the less donating bridging carboxylate group of each $NH_3^+–CH(\mathbf{R})–COO^-$ zwitterion. The observed trend of stability (GLY > ALA > PHE > VAL > LEU > PRO) is apparently related to the increasing steric repulsive effects exerted by the **R** substituent.

Then, it is useful to compare (see Fig. 11) the equilibrium constants for the $[Cu^{II}_2(\mathbf{8})]^{4+}$–AA interaction (bars), with the

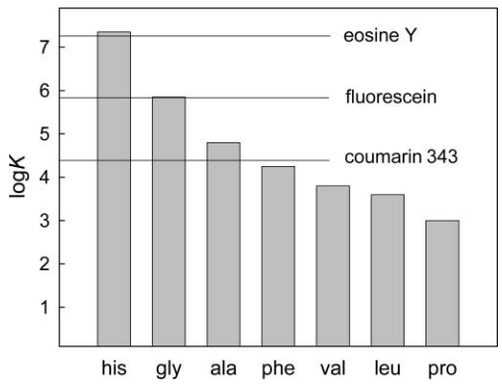

Fig. 11 Log K values for the binding interaction of the receptor $[Cu^{II}_2(\mathbf{8})]^{4+}$ with some natural amino acids (bars) and fluorescent indicators (horizontal lines). The position of the horizontal line with respect to the bars determines the selectivity of the $[Cu^{II}_2(\mathbf{8})]^{4+}$/indicator chemosensing duo towards the chosen amino acid.

equilibrium constants for the $[Cu^{II}_2(\mathbf{8})]^{4+}$–indicator binding (horizontal lines). Noticeably, the relative position of each line with respect to the bars accounts for the more or less selective behaviour illustrated in Fig. 10. In particular, discrimination requires that the binding constant of the indicator (horizontal line) is (i) distinctly lower than that of the amino acid of interest, and (ii) considerably higher than that of the interfering amino acid. This is not the case of coumarin, which cannot discriminate HIS and GLY (both exhibiting much higher association constants) and shows competitive behavior with ALA and PHE. On the other hand, the binding constant of fluorescein is significantly lower than that of HIS, but very close to that of GLY, which shows, therefore, competitive behavior. The more favourable situation – not the ideal one, however – for selective detection of HIS is observed with eosine Y, whose log K is sufficiently higher than that of any possible interferent, and is lower, even if slightly, than that of the analyte of interest.

Noticeably, the same chemosensing duo constituted by $[Cu^{II}_2(\mathbf{8})]^{4+}$ and one of the three previously considered fluorescent indicators (**10**, **11** or **12**) can be used to recognise inorganic anions acting as ambidentate, in particular for discriminating orthophosphate (Pi) and pyrophosphate (PPi).[19] In brief, Fig. 12 compares the binding constants of $[Cu^{II}_2(\mathbf{8})]^{4+}$ with PPi and Pi (bars) and with the association constants with the three indicators (horizontal lines).

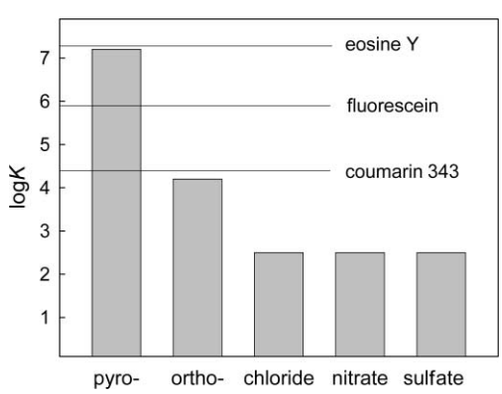

Fig. 12 Log K values for the binding interaction of the receptor $[Cu^{II}_2(\mathbf{8})]^{4+}$ with pyrophosphate, orthophosphate and other inorganic anion (bars) and with fluorescent indicators (horizontal lines). Log K for Cl^-, NO_3^- SO_4^{2-} is <3 and is set at 2 log units in the bar diagram, for sake of clarity.

The diagram in Fig. 12 immediately says that fluorescein is the ideal indicator for discriminating PPi from Pi, when operating with the $[Cu^{II}_2(\mathbf{8})]^{4+}$ receptor: in fact, the receptor/fluorescein binding constant is distinctly lower than the the receptor/PPi binding constant and is also markedly higher than

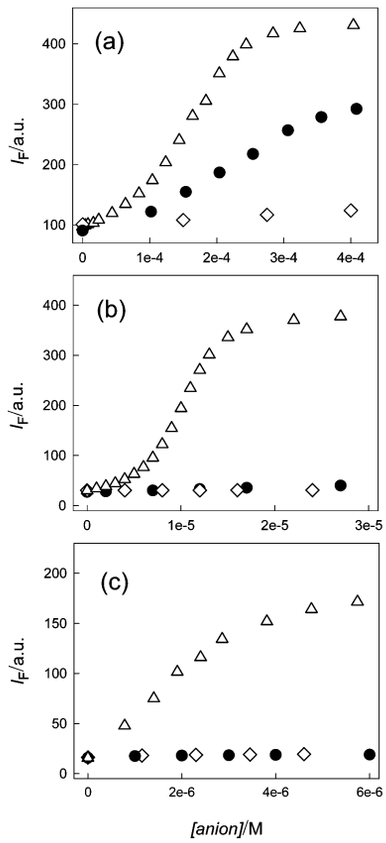

Fig. 13 Titration of the chemosensing ensemble $[Cu^{II}_2(\mathbf{8})]^{4+}$/indicator (In) in aqueous solution, at pH = 7, with pyrophosphate (△), orthophosphate (●), chloride, nitrate, sulfate (◇) : (a) In = coumarin 343: 10^{-6} M, $[Cu^{II}_2(\mathbf{8})]^{4+} = 2.5 \times 10^{-4}$ M; (b) In = fluorescein: 10^{-6} M, $[Cu^{II}_2(\mathbf{8})]^{4+} = 1.6 \times 10^{-5}$ M; (c) In = eosine Y: 10^{-6} M, $[Cu^{II}_2(\mathbf{3})]^{4+} = 2.4 \times 10^{-6}$ M.

the receptor/Pi association constant. This is confirmed by the titration profiles reported in Fig. 13(b), which show that PPi displaces fluorescein from the receptor (fluorescence ON) and Pi does not (fluorescence OFF).

Other common inorganic anions (Cl^-, NO_3^-, SO_4^{2-}), whose binding constant to $[Cu^{II}_2(\mathbf{8})]^{4+}$ is lower than 10^3, do not interfere, too. On the other hand, coumarin has a too low binding constant to $[Cu^{II}_2(\mathbf{8})]^{4+}$, only slightly higher than that of Pi. Thus, as shown in Fig. 13(a), Pi displays a competitive behaviour and generates interference. Conversely, eosine Y has a binding constant to $[Cu^{II}_2(\mathbf{8})]^{4+}$ higher, even if slightly, than that to PPi: as a consequence, PPi has some difficulty in displacing eosine Y from the receptor, thus generating a moderate reviving of fluorescence (see Fig. 13(c)).

At this stage, after the successful tests on selective sensing of histidine and pyrophosphate we can express our satisfaction with the 'Chemosensing Ensemble' paradigm, for three main reasons: (i) the recognition of the analyte of interest was signalled by fluorescence revival, rather than by quenching; (ii) a further element of selectivity was introduced in addition to that related to the mere receptor–analyte interaction: the choice of the indicator; (iii) the fluorophore was used as such (a commercial product) and had not to be covalently linked to the receptor, thus avoiding tedious and costly synthetic work.

In a more strictly chemical sense, we have appreciated the versatility of $[Cu^{II}_2(\mathbf{8})]^{4+}$ as a receptor, which was able to establish strong coordinative interactions with anions of diverse nature, like imidazolate and pyrophosphate: in particular, the two ambidentate anions exhibit rather different bite length (we intend for bite length the distance between the two coordinating donor atoms of the ligand), which for imidazolate is 2.33 Å, and for pyrophosphate is 4.52 Å. This may be due to the flexibility of the polyamine ring **8**, which can easily rearrange to

accommodate guests, whose size may vary substantially. It seems reasonable to predict that moving from a macrocycle to a macrotricycle, *i.e.* from a ring to a cage, the receptor framework is rigidified and guest accommodation must become more selective.

In this perspective, we considered the octamine cage **13**, which consists of two tren subunits, linked by 1,3-xylyl spacers, and can incorporate two metal ions in the tren cavities. It may happen that the cation, *e.g.* Cu^{II}, likes to be five-coordinate according to a trigonal bipyramidal geometry (an arrangement favoured by tren coordination), thus leaving one of its axial positions available for the donor atom of an ambidentate anion. Therefore, according to the cascade process illustrated in Fig. 14, the bis-tren cage **13** first incorporates two metal ions, to give $[Cu^{II}_2(\mathbf{13})]^{4+}$ (**14**), then includes an ambidentate anion X^-, to give $[Cu^{II}_2(\mathbf{13})(X)]^{3+}$ (**15**) (eqn. (5)). Crystal and molecular

$$[Cu^{II}_2(\mathbf{13})]^{4+} + X^- \rightleftharpoons [Cu^{II}_2(\mathbf{13})(X)]^{3+} \qquad (5)$$

structures have been reported, which demonstrated the complete encapsulation of polyatomic anions (*e.g.* N_3^-, NCO^-) within the dimetallic polyamine cage.[20]

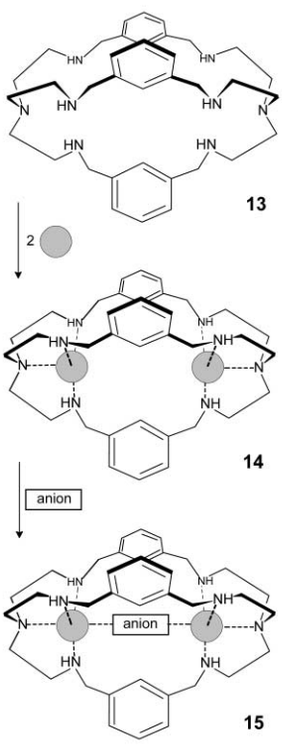

Fig. 14 A cascade process for the inclusion of an anion within a homodimetallic bis-tren complex. Each metal centre (*e.g.* Cu^{II}) wants to be five-coordinated (according to a trigonal bipyramidal geometry) and leaves one of its axial position available for the donor atom of an ambidentate anion. Inclusion selectivity depends on how the anion fits the intermetallic distance.

The constants for the anion inclusion equilibrium (5) in an aqueous solution at pH = 7, were determined spectrophotometrically for a series of inorganic anions of differing size and shape and were found to vary over about three orders of magnitude.[21]

The general behaviour can be rationalised in terms of bite length of the anion (as an example, the bite length of two selected anions: HCO_3^- and NCO^- are shown in Fig. 16). In particular, the plot of log *K* for the inclusion equilibrium (5) *vs.* anion bite length, reported in Fig. 15, displays peak selectivity: the highest stability (peak) is observed with the N_3^- anion, whose bite (2.33 Å) fits perfectly the distance of the two vacant positions on the Cu^{II} centres. The NCO^- and HCO_3^- anions

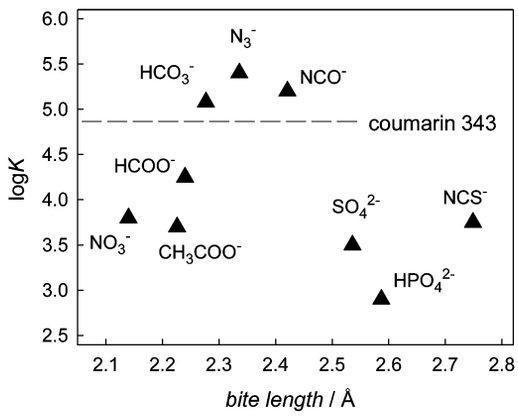

Fig. 15 Peak selectivity in the recognition of inorganic polyatomic anions by the dicopper(II) bis-tren receptor **14**. Log *K* values of inclusion constants were determined in an aqueous solution buffered at pH = 7. Bite length refers to the distance of the two coordinating donor atoms of the ambidentate anion. The dimetallic receptor recognises the bite of the anion and not its shape. The N_3^- ion provides the most favourable bite length (2.34 Å) to encompass the distance between the two vacant coordination sites of the two Cu^{II} centres. This diagram is reminiscent of the classical log *K vs.* ionic radius plots observed for the recognition of alkali metals by *crowns* and *cryptands*.

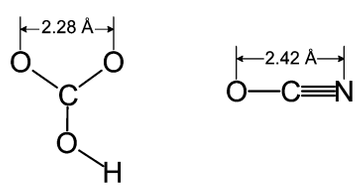

Fig. 16 Bite length of HCO_3^- and NCO^- anions, used in the diagram in Fig. 15. Distances were calculated through a semi-empirical method. These values were preferred to those taken from crystallographic studies, which can be altered by the electrostatic interactions with counterions.

exhibit a favourable, even if not ideal, bite length (2.42 and 2.28 Å, respectively) and show a good affinity for the $[Cu^{II}_2(\mathbf{13})]^{4+}$ receptor. Anions showing a longer (NCS^-, 2.75 Å) or a shorter bite (NO_3^-, 2.14 Å) give much less stable inclusion complexes: the lower stability reflects the endoergonic rearrangement the cage has to experience when it expands or reduces its cavity in order to include the anion.[22]

Among the three anions displaying peak affinity (HCO_3^-, N_3^- and NCO^-) we convey our interest on hydrogencarbonate, which is ubiquitous in the environment and whose analytical determination is important in many aspects. Thus, on the basis of the peak selectivity plot in Fig. 15, we want to design a chemosensing ensemble for HCO_3^-. In particular, we have to couple a fluorescent indicator to the $[Cu^{II}_2(\mathbf{13})]^{4+}$ receptor, in order to form a smart sensing duo. Among the currently used indicators, we chose coumarin 343, whose binding constant to the $[Cu^{II}_2(\mathbf{13})]^{4+}$ receptor is 4.8 log units. Very promisingly, this value (reported as a horizontal line in Fig. 15) is distinctly lower than the inclusion constant of HCO_3^- and sufficiently higher than the inclusion constants of other inorganic anions (nitrate, phosphate, sulfate). As a consequence, the chemosensing duo $[Cu^{II}_2(\mathbf{13})]^{4+}$/coumarin 343 results appropriate for the selective fluorescent detection of hydrogencarbonate. In fact, as shown in Fig. 17, titration of the $[Cu^{II}_2(\mathbf{13})]^{4+}$/coumarin 343 ensemble with HCO_3^- fully regenerates indicator emission, whereas titration with any other common inorganic anion leaves fluorescence quenched.

Thus, the $[Cu^{II}_2(\mathbf{13})]^{4+}$/coumarin 343 ensemble provides a fast and convenient procedure for detection of carbonate in water. Notice that the standard procedure for determination of carbonate in mineral water is based on a classical acid–base titration (which cannot discriminate other bases besides carbonate

present in solution). The fluorimetric procedure titrates specifically the HCO_3^- ion.

Finally, Fig. 18 pictorially illustrates the two sensing paradigms discussed above: the 'fluorophore–spacer–receptor' approach, (a), which operates through an ON OFF signalling mode, and the 'chemosensing ensemble' approach, (b), which signals recognition through the OFF ON switching of fluorescence.

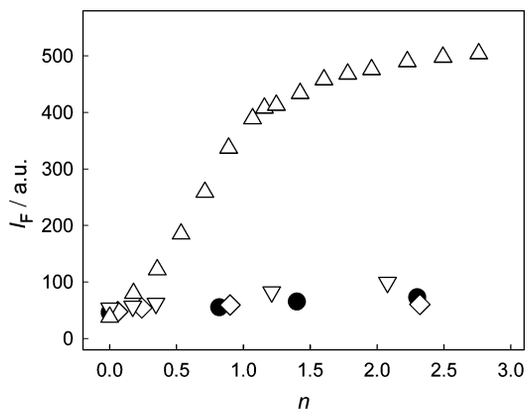

Fig. 17 Competitive titration of an aqueous solution 2×10^{-4} M in $[Cu^{II}_2(\mathbf{13})]^{4+}$ and 10^{-7} M in coumarin 343, buffered to pH = 7, with standard solutions of selected anions. HCO_3^- (△) is able to displace from receptor the indicator, which, released to the solution, displays its full emission. Other anions, *e.g.* phosphate (▽), acetate (●), sulfate (◇) do not compete successfully with $[Cu^{II}_2(\mathbf{13})]^{4+}$ for the indicator and induce only a slight fluorescence enhancement.

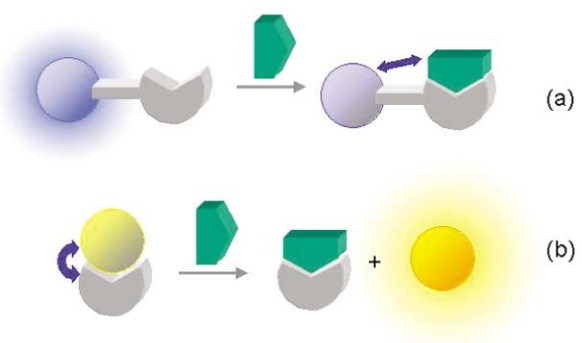

Fig. 18 The "fluorophore–spacer–receptor" paradigm, (a), and the "chemosensing ensemble" paradigm, (b).

Concluding remarks

This article reflects our own experience in the field of fluorescent chemosensors, and comments on how we approached the problem and we developed concepts and expertise.[23] As a consequence, the examples discussed come all from the work of our Laboratory. However, many researchers have recently designed and are currently designing fluorescent sensors for a variety of analytes, which includes s and d block cations, anions, molecules. In most cases the design is addressed to the fluorophore–spacer–receptor paradigm, probably because it has been the first to be developed. However, besides the signalling mode, which is matter of choice, the very important point is the design of the ideal receptor for the envisaged analyte, *i.e.* the synthesis of a system capable to establish strong and possibly selective interactions with the substrate of interest. We have tried to demonstrate that the metal–ligand interaction is the most appropriate and versatile for this type of study. Due to our personal experience in coordination chemistry, the examples discussed are related to the chemistry of metal complexes of multidentate amine ligands (open-chain, macrocycles, cages). However, coordination chemistry offers countless chances for the design of fluorescent sensors for any sort of analytes. We encourage coordination chemists to utilise their own experience for providing valuable receptors and sensors for ions and molecules of specific interest in medicine, biology and environmental chemistry.

References

1 A. Weller, *Pure Appl. Chem.*, 1968, **16**, 115.
2 G. De Santis, L. Fabbrizzi, M. Licchelli, A. Poggi and A. Taglietti, *Angew. Chem., Int. Ed. Engl.*, 1996, **35**, 202.
3 A. P. de Silva, H. Q. N. Gunaratne, T. Gunnlaugsson, A. J. M. Huxley, C. P. McCoy, J. T. Rademacher and T. E. Rice, *Chem. Rev.*, 1997, **97**, 1515.
4 R. A. Bissell, A. P. de Silva, H. Q. N. Gunaratne, P. L. M. Lynch, G. E. M. Maguire and K. R. A. S. Sandanayake, *Chem. Soc. Rev.*, 1992, 187.
5 L. Fabbrizzi, M. Licchelli, G. Rabaioli and A. Taglietti, *Coord. Chem. Rev.*, 2000, **205**, 8.
6 L. Fabbrizzi, M. Licchelli, A. Perotti, A. Poggi, G. Rabaioli, D. Sacchi and A. Taglietti, *J. Chem. Soc., Perkin Trans. 2.*, 2001, 2108.
7 W. Kaim and J. Rall, *Angew. Chem., Int. Ed. Engl.*, 1996, **35**, 43.
8 P. K. Coughlin, A. E. Martin, J. C. Dewan, E.-I. Watanabe, J. E. Bulkowski, J.-M. Lehn and S. J. Lippard, *Inorg. Chem.*, 1984, **23**, 1004.
9 Z.-W. Mao, Q.-W. Hang, W.-X. Tang, S.-X. Liu, Z.-M. Wang and J.-L. Huang, *Polyhedron*, 1996, **15**, 321.
10 L. Fabbrizzi, G. Francese, M. Licchelli, A. Perotti and A. Taglietti, *Chem. Commun.*, 1997, 581.
11 L. Fabbrizzi, M. Licchelli, A. Taglietti and M. Zema, unpublished results.
12 F. P. Schmidtchen and M. Berger, *Chem. Rev.*, 1997, **97**, 1609.
13 F. Grohovaz, San Raffaele Hospital, Milan, personal communication to L. F.
14 M. J. Perry, in *Monoclonal Antibodies: Principles and Applications*, ed. J. R. Birch and E. S. Lennox, Wiley–Liss, New York, 1995, pp. 107–120.
15 S. L. Wiskur, H. Aït-Haddou, J. J. Lavigne and E. V. Anslyn, *Acc. Chem. Res.*, 2001, **34**, 963.
16 L. Fabbrizzi, M. Licchelli, P. Pallavicini, A. Perotti, A. Taglietti and D. Sacchi, *Chem.–Eur. J.*, 1996, **2**, 75.
17 H.-L Zhu, Q.-W Hang, J. Zhao, C.-Y Duan and W.-X. Tang, *Transition Met. Chem.*, 1999, **24**, 131.
18 M. A. Hortalá, L. Fabbrizzi, N. Marcotte, F. Stomeo and A. Taglietti, *J. Am. Chem. Soc.*, 2003, **125**, 20.
19 L. Fabbrizzi, N. Marcotte, F. Stomeo and A. Taglietti, *Angew. Chem., Int. Ed.*, 2002, **41**, 3811.
20 C. J. Harding, F. E. Mabbs, E. J. L. MacInnes, V. McKee and J. Nelson, *J. Chem. Soc., Dalton Trans.*, 1996, 3227.
21 L. Fabbrizzi, A. Leone and A. Taglietti, *Angew. Chem., Int. Ed.*, 2001, **40**, 3066.
22 L. Fabbrizzi, P. Pallavicini, A. Perotti, L. Parodi and A. Taglietti, *Inorg. Chim. Acta*, 1995, **238**, 5.
23 L. Fabbrizzi and A. Poggi, *Chem. Soc. Rev.*, 1995, **24**, 197.